Science in China Series E: Technological Sciences

www.scichina.com
tech.scichina.com
www.springerlink.com

Frequency-domain analysis of computer-controlled optical surfacing processes

ZHOU Lin†, DAI YiFan, XIE XuHui & LI ShengYi

College of Mechatronic Engineering and Automation, National University of Defense Technology (NUDT), Changsha 410073, China

Mid-high spatial frequency errors are often induced on optical surfaces polished by computer-controlled optical surfacing (CCOS) processes. In order to efficiently remove these errors, which would degrade the performances of optical systems, the ability of a CCOS process to correct the errors have been investigated based on the convolution integral model in view of the availability of material removal. To quantify the ability, some conceptions, such as figure correcting ability and material removal availability (MRA), have been proposed. The research result reveals that the MRA of the CCOS process to correct a single spatial frequency error is determined by its tool removal function (TRF), and it equals the normalized amplitude spectrum of the Fourier transform of its TRF. Finally, three sine surfaces were etched using ion beam figuring (IBF), which is a typical CCOS process. The experimental results have verified the theoretical analysis. The employed method and the conclusions of this work provide a useful mathematical basis to analyze and optimize CCOS processes.

computer-controlled optical surfacing (CCOS), optics machining, tool removal function (TRF), material removal availability (MRA), ion beam figuring (IBF)

Employing a small computer-controlled tool to polish optics is a breakthrough technology for optics machining. This new technology is often called computer-controlled optical surfacing (CCOS). This method was proposed by Itek inc. in the 1970s[1]. At that time, the CCOS technology only referred to the computer controlled polishing (CCP) technique which uses a small lap to polish. Now, several other CCOS techniques have been developed, such as magnetorheological finishing (MRF)[2], ion beam figuring (IBF)[3], stressed-lap polishing (SLP)[4], bonnet tool polishing (BTP)[5], and fluid jet polishing (FJP)[6]. All these techniques employ a computer-controlled tool to polishing. The tool is sufficiently smaller than the optics being polished such that only a local surface can be polished at a time. The longer the tool dwells at a local, the more material is removed. The small tool is controlled to scan the optical surface at varying velocities or at varying dwell times to correct the optical surface error by selectively removing local material. All these CCOS techniques can be mathematically modeled and the processes are deterministic. Hence, a CCOS process is also called a deterministic polishing process. The applications of CCOS processes have largely increased the efficiency of optics machining. Today, CCOS technologies are more and more employed to machining optics. Almost all famous optics manufacturers in the world have applied CCOS techniques, such as the Optical Sciences Center at University of Arizona, the Center for Optics Manufacturing (COM) at University of Rochester, Itek Inc., Tinsley Inc., Lawrence Livermore National Laboratories (LLNL), Eastman Kodak Company, QED Technologies, University College of London (UCL), Zeeko Inc., ROSEC Lab., Vavilov State Optical Institute, Zeiss Inc., and Cannon Inc..

However, due to the application of the small tool, it often induces more mid-high spatial frequency errors on

Received October 11, 2007; accepted October 13, 2008
doi: 10.1007/s11431-009-0111-7
†Corresponding author (email: zhoulin_cn@nudt.edu.cn, zhoulin_cn@sohu.com)
Supported by the National Basic Research Program of China (“ 973” Project) and the National Natural Science Foundation of China (Grant No. 50775215)

the optical surfaces polished by CCOS processes[7]. These mid-high spatial frequency errors would degrade the performances of the precision optical systems, such as intense laser systems, shortwave optical systems and high resolution imaging systems[8]. Therefore, these errors should be considered and removed from the CCOS processes[9]. Based on the convolution integral model, which is widely applied in CCOS processes, this study investigates the ability of a CCOS process to correct the errors in view of the availability of material removal. Finally, some experiments have been performed to prove the theoretical analysis.

1 Convolution integral model

A general flowchart of a complete CCOS process is illustrated in Figure 1. First, a particular experiment should be performed to obtain the material removal distribution of the polishing tool in a unit time, which is referred to as the tool removal function (TRF) or the influence function (IF)[10]. And the optical surface should be measured and the error contour of it should be calculated also. Then, based on the obtained TRF and the error contour, the dwell time will be calculated from a specific dwell-time algorithm. Finally, the optics will be processed according to the calculated dwell time under the same parameters to the TRF experiment.

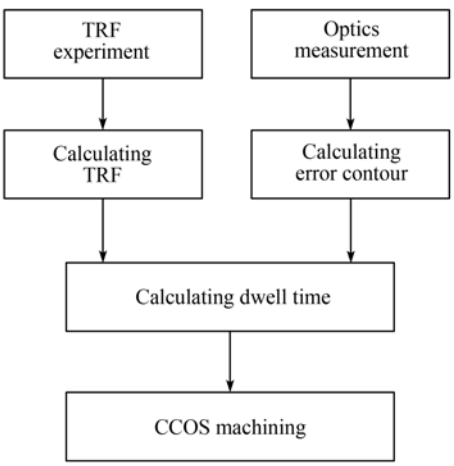

Figure 1 General flowchart of a complete CCOS process.

Suppose the TRF is invariant in time and space, the total material removal of a CCOS process can be calculated from the convolution integral of the dwell time and the TRF[11,12] as follows

$$r(x,y)=\tau(x,y)\otimes p(x,y), \tag{1}$$

where $r(x, y)$ is the total material removal, $\tau(x, y)$ is the dwell time, and $p(x, y)$ is the TRF of the process, $\otimes$ stands for the convolution operator. Therefore, the calculation of dwell time from the error contour and the TRF is a deconvolution process according to eq. (1).

It is well known that a convolution integral operation in the time-domain or spatial-domain can be calculated by a multiplication operation in the frequency-domain. Then eq. (1) becomes

$$R(u,v)=T(u,v)\cdot P(u,v), \tag{2}$$

where $R(u, v)$, $T(u, v)$ and $P(u, v)$ stand for the two-dimensional Fourier transforms (FT) of $r(x, y)$, $\tau(x, y)$ and $p(x, y)$, respectively. From this equation, we get

$$T(u,v)=\frac{R(u,v)}{P(u,v)}. \tag{3}$$

It can be seen that the model of a CCOS process is the same as the model of a linear time invariant (LTI) system. Both can be modeled with a convolution integral formulation. Therefore, a CCOS process can be regarded equivalent to an LTI system. The TRF $p(x, y)$, the dwell time $\tau(x, y)$ and the material removal $r(x, y)$ in a CCOS process are equivalent to the unit impulse response function, the input signal and the output signal, respectively. Consequently, to calculate the dwell time in a CCOS process is equivalent to determine the input signal based on the output signal and the unit impulse response function.

2 Theoretical analysis

2.1 Universal formulation

Although a CCOS process is equivalent to an LTI system, it has some characteristics different from an LTI system. For example, the dwell time must be non-negative, while the input of an LTI system can be negative. To analyze its specific characteristics, a CCOS process to correct an error surface of a single spatial frequency is first considered.

Suppose the error surface to be corrected is

$$r_e(x,y)=A_e\cdot\sin\left[2\pi\left(f_x x+f_y y\right)\right]. \tag{4}$$

It describes a sine surface on the x-y plane, with amplitude A_e, frequency on x direction f_x, and frequency on y direction f_y. Based on the convolution integral model, the dwell time used to correct this sine error can be cal-

culated as (For more details please see Appendix)

$$\tau_e(x,y)=\frac{A_e}{\left|P\left(f_x,f_y\right)\right|}\sin\left[2\pi\left(f_x x+f_y y\right)-\varphi\left(f_x,f_y\right)\right], \quad (5)$$

where $P(f_x, f_y)$ is the value of the $P(u,v)$ at the frequency (f_x, f_y). $|P(f_x, f_y)|$ and $\varphi(f_x, f_y)$ stand for the amplitude and the phase of the $P(f_x, f_y)$, respectively, i.e., $P(f_x, f_y)=|P(f_x, f_y)|\cdot e^{i\varphi(fx,fy)}$.

Since the process time must be non-negative, the dwell time $\tau_e(x, y)$ should be offset to a non-negative dwell time. The final offset non-negative dwell time $\tau_a(x, y)$ is

$$\tau_a(x,y)=\tau_e(x,y)+\frac{A_e}{\left|P\left(f_x,f_y\right)\right|}. \quad (6)$$

Based on the convolution integral model, the actual material removal $r_a(x, y)$ can be calculated form the above actual dwell time as

$$r_a(x,y)=\tau_a(x,y)\otimes p(x,y)=r_e(x,y)+\frac{A_e B}{\left|P\left(f_x,f_y\right)\right|}, \quad (7)$$

where $B=\int_{-\infty}^{\infty}\int_{-\infty}^{\infty}p(x,y)\mathrm{d}x\mathrm{d}y$. It is the integral of the TRF, and it physically describes the volume removal rate of the process.

It can be seen from eq. (7) that the amplitude of the actual material removal is $A_eB/|P(f_x, f_y)|$, while the amplitude of the error is A_e. On the other hand, we have $|P(f_x, f_y)|\leqslant B$ according to the properties of the FT. Thus, $A_eB/|P(f_x, f_y)|\geqslant A_e$. This means that the material removal in a real process is more than the desired material removal. As a passive LTI system will damp the amplitude of the input signals, a CCOS process will damp the amplitude of the input with removing additional uniform material. The ratio of the desired material removal to the actual material removal is defined as the material removal availability (MRA) ε in our study

$$\text{Material removal availability}\ \varepsilon=\frac{\text{Desired material removal}}{\text{Actual material removal}}. \quad (8)$$

According to this definition, we have $0\leqslant\varepsilon\leqslant1$. For a CCOS process to correct a specific error, the stronger the ability of the process to correct the error is, the less the total actual material removal and the higher the MRA value. Contrarily, the weaker the ability to correct the error is, the more the total actual material removal, and the lower the MRA value. Therefore, the ability of the process to correct errors can be quantificationally evaluated by its MRA value, and can be also called the figure correcting ability value. The sketch of the material removals in a typical CCOS process is illustrated in Figure 2.

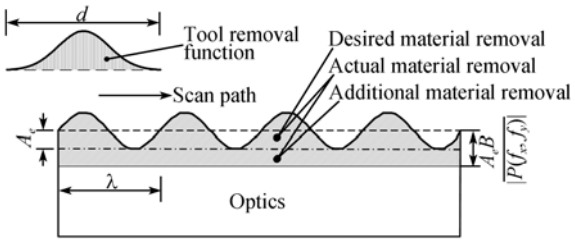

Figure 2 Sketch of the material removals in CCOS processes.

Based on the definition of the MRA and the above analysis, the MRA of a CCOS process to correct an error surface of a single spatial frequency (f_x, f_y) is

$$\varepsilon\left(f_x,f_y\right)=\frac{A_e}{\frac{A_eB}{\left|P\left(f_x,f_y\right)\right|}}=\frac{1}{B}\left|P\left(f_x,f_y\right)\right|. \quad (9)$$

Eq. (9) shows that the MRA of a CCOS process is determined by its TRF, and it just equals the normalized amplitude spectrum of the FT of its TRF. Eq. (9) can also be expressed in a polar form

$$\varepsilon\left(f,\theta\right)=\frac{1}{B}\left|P\left(f,\theta\right)\right|. \quad (10)$$

It explicitly shows that the MRA values vary depending on both the amplitude and the direction of the error spatial frequency.

The above analysis does not refer to a specific CCOS technology, or a specific TRF, therefore, the formulations of eqs. (9) and (10) universally satisfy all CCOS technologies, such as CCP, MRF and IBF, and also satisfy all shape TRFs, regardless whether it is rotationally symmetric.

2.2 Special cases

The above analysis shows that the MRA varies depending on both the amplitude and the direction of the error spatial frequency. However, in the following two familiar cases, the MRA varies on only the amplitude and can be calculated with simple formulations.

2.2.1 Process with rotationally symmetric TRF. The TRFs of most CCOS processes, such as CCP and IBF, are rotationally symmetric. For a process with a rotationally symmetric TRF, the figure correcting abilities in

different directions are identical. Therefore the MRA is only a function of the frequency amplitude. In this case, the MRA can be expressed as $\varepsilon(f)$ and can be calculated using the following equation

$$\varepsilon(f)=\frac{1}{B_p}\left|F\{p(r)\}\right|, \tag{11}$$

where $p(r)$ is the generatrix of the rotationally symmetric TRF, and $B_p=\int_{-\infty}^{\infty}p(r)\mathrm{d}r$. Eq. (11) shows that the MRA of a process with a rotationally symmetric TRF just is equals the normalized amplitude spectrum of the FT on the generatrix.

2.2.2 One-dimensional process. One-dimensional process means a process with its surface error (and consequently the dwell time) varying only in a spatial direction. Suppose the error varies only along the x direction, i.e., the spatial frequency(f_x, f_y) can be expressed as $(f, 0)$. In this case, the MRA is also only a function of the frequency amplitude f. Therefore, the MRA can be expressed as $\varepsilon(f)$, and can be calculated using the following equation

$$\varepsilon(f)=\frac{\left|P(f,0)\right|}{B}=\frac{1}{B}\left|F\{p_x(x)\}\right|, \tag{12}$$

where $p_x(x)$ stands for one-dimentional TRF, which is defined as $p_x(x)=\int_{-\infty}^{\infty}p(x,y)\mathrm{d}y$. Eq. (12) shows that the MRA of a one-dimensional process just equals the normalized amplitude spectrum of the FT of its corresponding one-dimensional TRF.

3 Experiments

3.1 Design of experiments

Experiments of correcting sine error surfaces can be performed. Therefore, the actual MRA values of experiments can be calculated and can be used to validate the theoretically predicted values. According to the knowledge of LTI system and the definition of the MRA, to correct a sine surface, the dwell time should also be a sine with the same spatial frequency. Furthermore, the amplitude of the sine error surface A_e, the amplitude of the actual material removal A_a, the amplitude of the dwell time A_τ and the MRA value ε satisfy the following relation

$$A_e=\varepsilon A_a=\varepsilon B A_\tau. \tag{13}$$

Suppose the sine error locates along the x direction; then the MRA value can be calculated using the eq. (12). Eq. (12) also shows that to calculate the MRA values just needs the one-dimentional TRF. To obtain the experimental one-dimentional TRF, the line scanning experiment[13] can be employed.

We have noticed that the ability of a process to correct a sine surface is the same as the ability to etch a sine profile from a plane, because their material removals in the processes are the same. However, the preparation of a fine sine surface is more difficult than the preparation of a fine plane. Therefore, the experiments of etching sine surfaces from plane surfaces will be performed instead of correcting prepared sine surfaces.

Since an IBF process is a highly deterministic CCOS process with a highly stable TRF[3], to increase the reliability of experiments, the IBF process is chosen to etch sine surfaces. The following experiments were performed on the IBF system, KDIFS-500, developed by NUDT[3]. The interferometer used to measure the surfaces was developed by Nanjing Technology University.

3.2 TRF experiment

The line scanning experiment[13] was performed on a Zurodur sample of a 100 mm diameter to obtain the one-dimensional TRF of the process. The surface contours of the sample before and after the experiment are shown in Figures 3(a) and (b), respectively. From the surface contours, the material removal in the process and the corresponding one-dimensional TRF can be calculated, as shown in Figures 3(c) and (d), respectively. With the calculated one-dimensional TRF, the MRA values of different frequencies can be calculated using eq. (12). The results are shown in Figure 3(e).

3.3 Etching sine surfaces

In the experiments, three sine surfaces with different wavelengths were etched from plane surfaces. Their wavelengths were 70, 40 and 20 mm, and the corresponding frequencies were 0.0143, 0.025 and 0.05 mm^{-1}, respectively. Figure 3(e) shows that the theoretical calculated MRA values of these processes are 0.566, 0.145 and 0.0084, respectively.

The input dwell time in each experiment was a sine of 0.011 $\mathrm{min}\cdot\mathrm{mm}^{-2}$ amplitude. The corresponding amplitude of the actual material removal was 1 μm according to the volume removal rate of the resulted one-dimensional TRF.

The processing parameters in these experiments were the same as those in the TRF experiment. The experimental results are shown in Figures 4, 5 and 6, respec-

tively. To reduce the processing time, the full sine surface was only etched in a strap of 8 mm width (see Figures 4(b), 5(b) and 6(b)). The average line profiles of the etched sine surfaces on the 8 mm strap were calculated and were shown in Figures 4(e), 5(e) and 6(e), respectively. Their amplitudes were calculated as 0.607, 0.147 and 0.0111 μm by a least-square fit. Therefore, their actual MRA values are 0.607, 0.147 and 0.0111 because their amplitudes of the input actual material removals are 1μm. The results are summarized in Table 1.

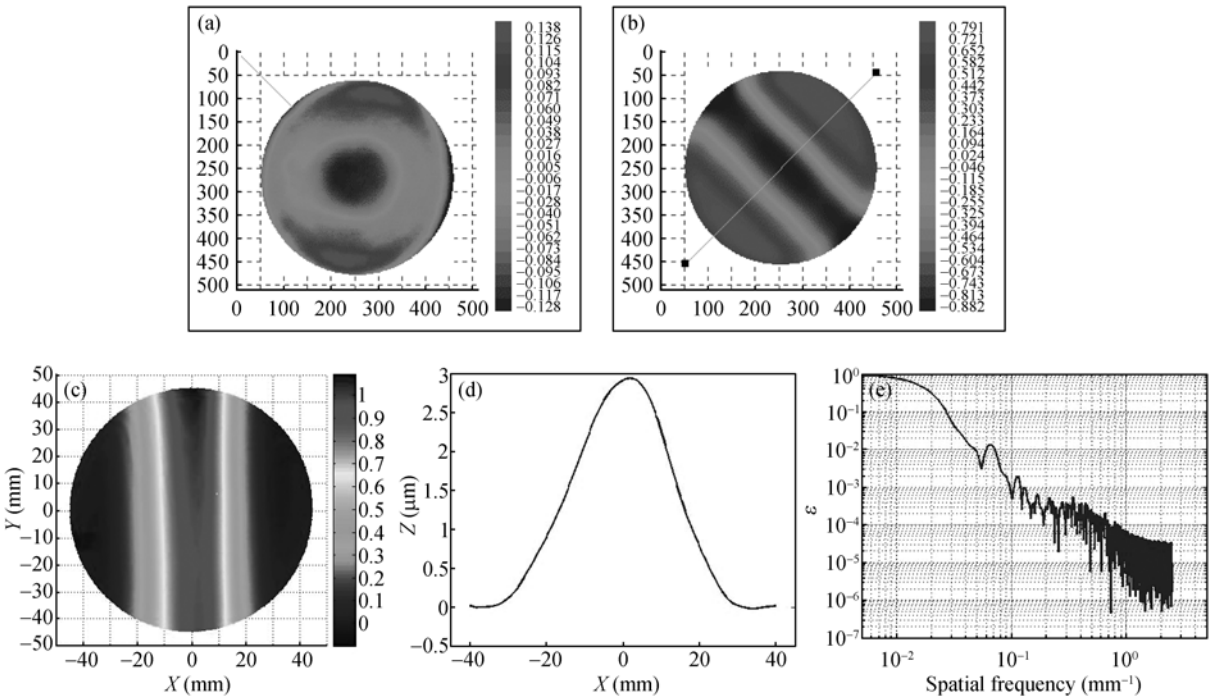

Figure 3 The BRF experimental results. (a) Surface contour before experiment; (b) surface contour after experiment; (c) resulted material removal (after rotation of –45º); (d) calculated one-dimensional TRF; (e) calculated MRA values vs. spatial frequencies.

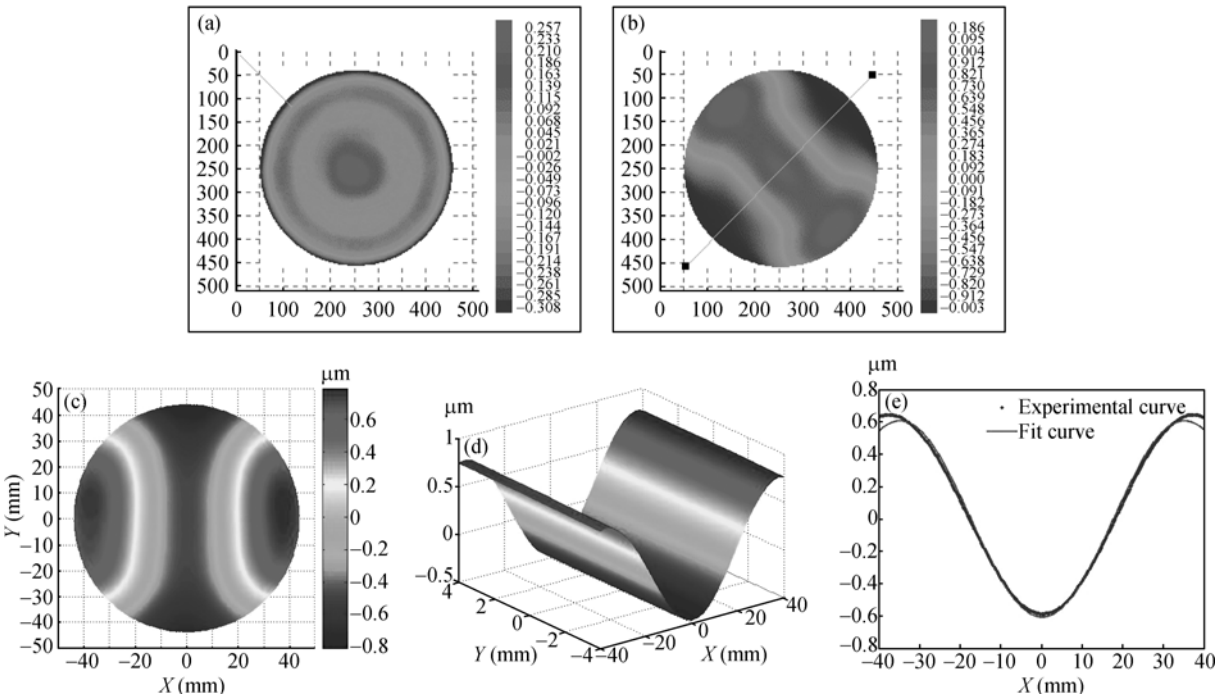

Figure 4 Experimental result of sine surface (70 mm wavelength). (a) Surface contour before experiment; (b) surface contour after experiment; (c) resulted material removal (after rotation –45º); (d) etched sine strap; (e) average line profile of the etched sine surface (0.607 μm amplitude).

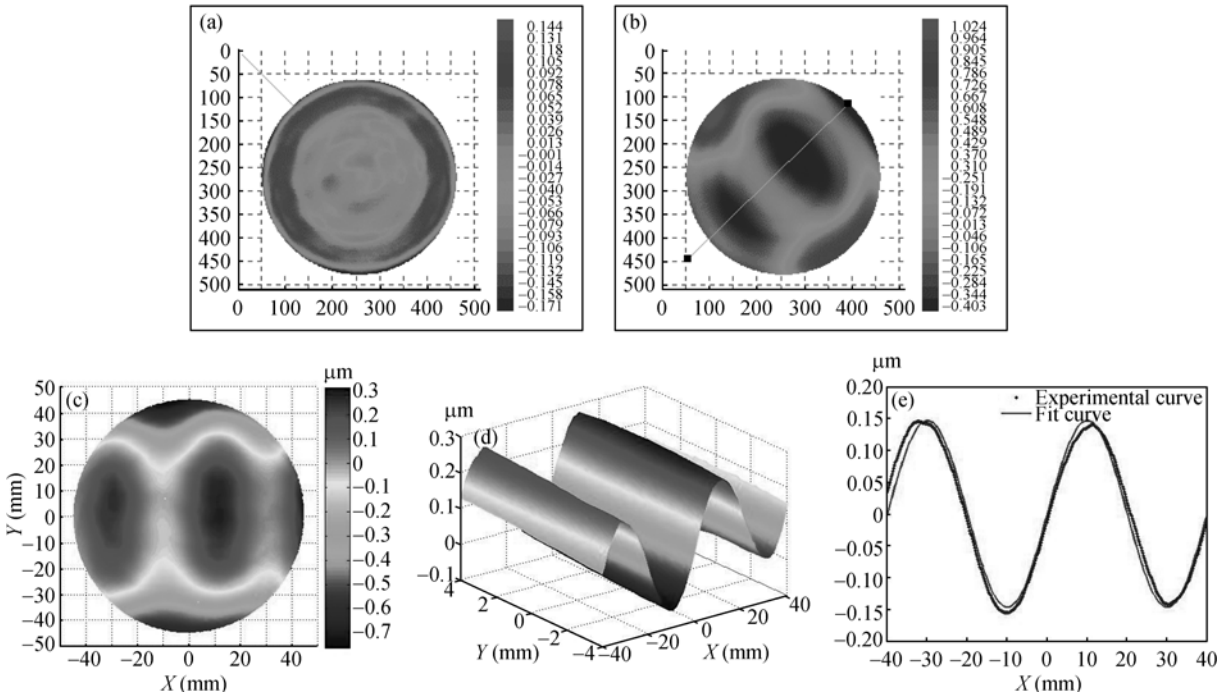

Figure 5 Experimental result of sine surface (40 mm wavelength). (a) Surface contour before experiment; (b) surface contour after experiment; (c) resulted material removal (after rotation –45º); (d) etched sine strap; (e) average line profile of the etched sine surface (0.147 μm amplitude).

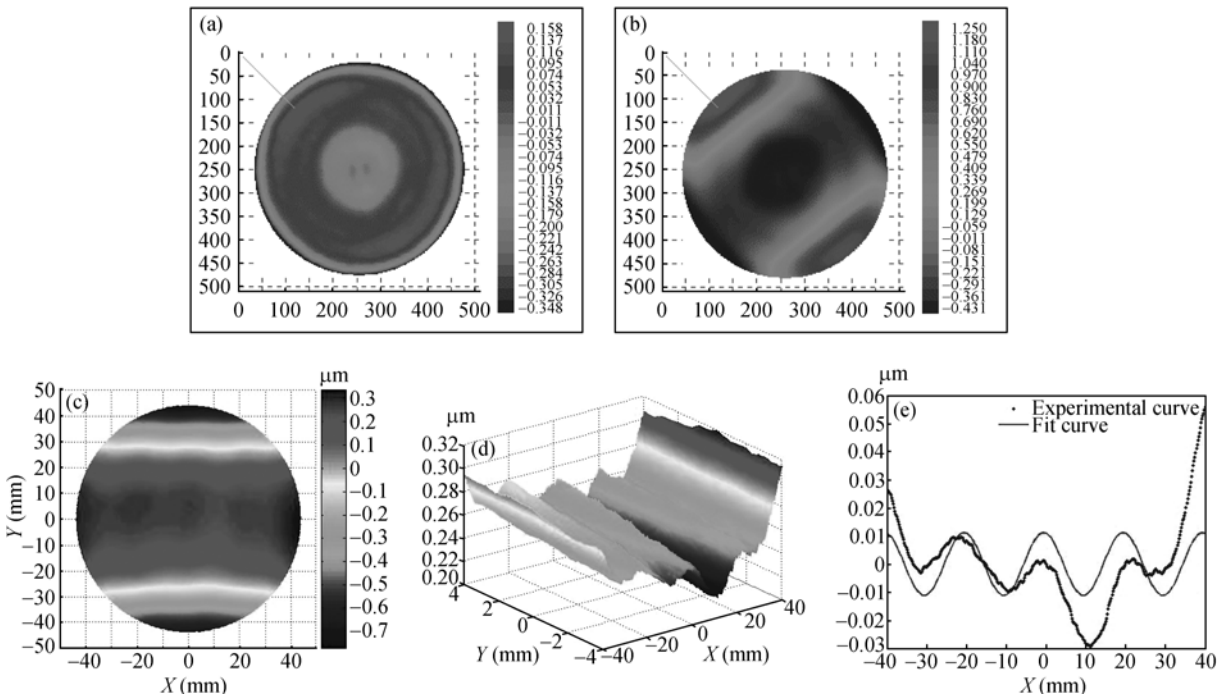

Figure 6 Experimental result of sine surface (20 mm wavelength). (a) Surface contour before experiment; (b) surface contour after experiment; (c) resulted material removal (after rotation –45º); (d) etched sine strap; (e) average line profile of the etched sine surface (0.0111 μm amplitude).

Table 1 The experimental results

Wavelength (mm)	70	40	20
Predicted MRA	0.566	0.145	0.0084
Actual MRA	0.607	0.147	0.0111
Deviation	7%	1%	32%

3.4 Results analysis

Table 1 shows that the MRA values of an actual process are generally consistent with the theoretical predicted MRA values. The largest deviation in the experiment of 20 mm wavelength might result from the measurement

errors due to its small amplitude. The experimental results also show that the resulted amplitude of a process with a large MRA value is greater than the amplitude of a small MRA value, although their input amplitudes of dwell times are identical.

4 Discussion

Based on the above analysis and the experimental results, it can be found that the ability of a CCOS process to correct the errors of mid-high spatial frequency can be evaluated by the MRA value. A CCOS process with a small MRA value can not effectively correct the errors. Experiments have shown that an IBF process with MRA value less than 0.1 could not effectively correct errors[14]. Therefore, in order to effectively correct the errors, the MRA value should be evaluated and optimized before the process improves the machining availability. For a specific error surface, the MRA of the error dominant frequency on different available technologies and different process parameters should be evaluated and optimized to increase the MRA.

For the processes with non-rotation symmetric TRF, such as MRF process, the direction of the dominant frequency on the error surface should coincide with the direction of the greatest MRA value to increase the machining availability.

Furthermore, a process with a smaller TRF diameter often indicates a higher MRA value. Therefore, to improve the ability of correcting the mid-high spatial frequency errors, reducing the diameter of the TRF is an effective way[15].

5 Conclusions

As a passive LTI system will damp the amplitude of the input signal, a CCOS process will damp the amplitude of the input also. It induces an additional uniform material removal, and causes the actual material removal is always more than the desired. The ratio of the desired material removal to the actual material removal is defined as MRA and its value reveals the ability of a process to correct errors. The values of MRA are between zero and one. The closer is the MRA value of a process to one, the less additional material will be removed, and the stronger ability of the process to correct errors.

The MRA value of a process to correct an error surface of a single spatial frequency varies depending on both the amplitude and the direction of the error frequency. The MRA value of a process is determined by its TRF, and it is just equal to the normalized amplitude spectrum of the FT of its TRF. The MRA value of a process with a rotationally symmetric TRF varies depending on only the amplitude of the error frequency, and it just equals the normalized amplitude spectrum of the FT of its generatrix function. The MRA value on the processing direction of a one-dimensional process varies depending on only the amplitude of the error frequency also, and it equals the normalized amplitude spectrum of the FT of the one-dimensional TRF.

Since the ability of a CCOS process to correct mid-high spatial frequency errors can be evaluated by the MRA value, and a process with a small MRA value can not correct the errors effeciely. Therefore, to improve the correcting ability of a process, the MRA values on different available CCOS techniques and different processing parameters should be evaluated and optimized to increase the MRA value.

Appendix

The sine surface described by eq. (4) can be expressed as a imaginary component of a complex:

$$r_e(x,y) = \mathrm{Im}\left[A_e \mathrm{e}^{\mathrm{i}2\pi(f_x x + f_y y)}\right], \tag{A1}$$

where $\mathrm{i} = \sqrt{-1}$. For convenience, the operator for imaginary component can be neglected. Thus we get

$$r_e(x,y) = A_e \mathrm{e}^{\mathrm{i}2\pi(f_x x + f_y y)}. \tag{A2}$$

The purpose of using complex is to replace the trigonometric functions with exponential functions, which are simple in calculations. This technique has been already used to handle signals. After the substitution, FT of the complex error surface $R_e(u, v)$ is

$$R_e(u,v) = A_e \cdot \delta(u - f_x, v - f_y), \tag{A3}$$

where $\delta(u, v)$ stands for a unit impulse function.

Thus, the FT of the dwell time $T_e(u, v)$ used to correct this error surface can be calculated from eq. (3)

$$T_e(u,v) = \frac{R_e(u,v)}{P(u,v)} = \frac{A_e}{P(f_x, f_y)}\delta(u - f_x, v - f_y). \tag{A4}$$

The corresponding dwell time $\tau_e(x, y)$ is

$$\tau_e(x,y) = F^{-1}\{T_e(u,v)\} = \frac{A_e}{P(f_x, f_y)}\mathrm{e}^{\mathrm{i}2\pi(f_x x + f_y y)}, \tag{A5}$$

where $F^{-1}\{\bullet\}$ is the operator for inverse FT. As the complex $P(f_x, f_y)$ can be expressed in polar form:

$$P(f_x, f_y) = \left|P(f_x, f_y)\right| \cdot \mathrm{e}^{\mathrm{i}\varphi(f_x, f_y)}, \tag{A6}$$

the dwell time of eq. (A5) becomes

$$\tau_e(x, y) = \frac{A_e}{\left|P(f_x, f_y)\right|} \mathrm{e}^{\mathrm{i}\left[2\pi(f_x x + f_y y) - \varphi(f_x, f_y)\right]}. \tag{A7}$$

Due to the linear properties of the above operations, the actual dwell time is the corresponding imaginary component of the result. Therefore, the final calculated dwell time is

$$\tau_e(x, y) = \frac{A_e}{\left|P(f_x, f_y)\right|} \sin\left[2\pi(f_x x + f_y y) - \varphi(f_x, f_y)\right]. \tag{A8}$$

1 Jones R A. Optimization of computer controlled polishing. Appl Opt, 1977, 16(1): 218－224[doi]

2 Zhang F, Yu J C, Zhang X J. Magnetorheological finishing technology (in Chinese). Opt Precision Eng, 1999, 7(5): 1－7[doi]

3 Dai Y F, Zhou L, Xie X H, et al. Realization of deterministically figuring in optics machining by ion beam (in Chinese). Acta Opt Sinica, 2008, 28(6): 1131－1135

4 Fan B, Wan Y J, Chen W, et al. Manufacturing features comparing between computer control active-lap and computer control optical surface for large aspheric optics (in Chinese). Chin J Lasers, 2006, 33(1): 128－132

5 Gao B, Yao Y X, Xie D G, et al. Movement modeling and simulation of precession mechanisms for bonnet tool polishing (in Chinese). Chin J Mech Eng, 2006, 42(2): 101－104

6 Guo P J, Fang H, Yu J C. Research on material removal mechanism of fluid jet polishing (in Chinese). Laser J, 2008, 29(1): 25－27

7 Bielke A, Bechstette K, Kübler C. Fabrication of aspheric optics-process challenges arising from a wide range of customer demands and diversity of machine technologies. In: Proceedings of SPIE. SPIE, 2004, 5252: 1－12

8 Taylor J S, Sommargren G E, Sweeney D W, et al. Fabrication and testing of optics for EUV projection lithography. In: Proceedings of SPIE. SPIE, 1998, 3331: 580－590[doi]

9 Lawson J K, Worfe C R, Manes K R, et al. Specification of optical components using the power spectral density function. In: Proceedings of SPIE. SPIE, 1995, 2536: 38－50[doi]

10 Schinhaerl M, Rascher R, Stamp R, et al. Utilisation of time-variant influence functions on the computer controlled polishing. Prec Eng, 2008, 32(1): 47－54[doi]

11 Drueding T W, Bifano T G, Fawcett S C. Contouring algorithm for ion figuring. Prec Eng, 1995, 17(1): 10－21[doi]

12 Cheng H B, Sun G Z, Feng Z J. Solving the input data in error corrction of optical fabrication by finite Fourier coefficient algorithm. Sci China Ser E-Tech Sci, 2006, 49(1): 50－60

13 Zhou L, Xie X H, Dai Y F, et al. Ion beam figuring system in NUDT. In: Proceedings of SPIE. SPIE, 2007, 6722: 67224A-1－67224A-6

14 Zhou L. Study on Theory and Technology in Ion Beam Figuring for Optical Surfaces (in Chinese). Dissertation of Doctoral Degree. Changsha: National University of Defense Technology, 2008. 4

15 Ghigo M, Canestrari R, Spiga D, et al. Correction of high spatial frequency errors on optical surfaces by means of ion beam figuring. In: Proceedings of SPIE. SPIE , 2007, 6671: 667114[doi]